Development of YAG:Ce,Mg and YAGG:Ce Scintillation Fibers

V. Kononets[1], K. Lebbou[2], O. Sidletskiy[1(✉)], Yu. Zorenko[3,4], M. Lucchini[5], K. Pauwels[5,6], and E. Auffray[5]

[1] Institute for Scintillation Materials, NAS of Ukraine, Kharkiv, Ukraine
sidletskiy@isma.kharkov.ua
[2] Institute of Light and Matter, UMR5306 CNRS, Universite de Lyon 1, Villeurbanne Cedex, France
[3] Institute of Physics, Kazimierz Wielki University in Bydgoszcz, Bydgoszcz, Poland
[4] Department of Electronics, Ivan Franko National University of Lviv, Lviv, Ukraine
[5] European Organization for Nuclear Research, Geneva 23, Switzerland
[6] University of Milano-Bicocca, Milan, Italy

Abstract. The chapter overviews the status of works on fabrication of long garnet fibers for application in high energy physics experiments. $Y_3Al_5O_{12}$:Ce, Mg (YAG:Ce,Mg) and $Y_3Al_{5-x}Ga_xO_{12}$:Ce (YAGG:Ce) fibers are grown by the μ-PD method. The scintillation and optical parameters of fibers are controlled by optimization of concentration of isovalent (Ga^{3+}) and aliovalent (Mg^{2+}) codoping, as well as by choice of growth parameters.

1 Introduction

A need for fiber-shaped scintillation detectors has arisen recently. Their possible applications include high-granularity detectors for high-energy physics (HEP) experiments [1–3], as well as detectors for well logging probes [4]. Micro-pulling-down (μ-PD) is among the most suitable methods to obtain crystal fibers of reviewed shape avoiding additional mechanical treatment. Accounting for peculiarities of crystallization of bulk crystals by the Czochralski and Bridgman methods, micro-PD at present is the only method to produce long (>20 cm) crystal fibers with uniform longitudinal activator distribution. In particular, a technology to produce long fibers of high-melting-temperature oxide crystals by the micro-PD is well developed in ILM (Lyon, France) [5].

Ce-doped rare-earth garnet scintillators are among the candidates for new HEP experiments at future colliders due to good mechanical properties, high light yield and fast luminescence response. In recent several years the engineering of crystals with garnet structure became a one of major trends in search for new efficient scintillation materials. Ce- and Pr-doped $Y_3Al_5O_{12}$:Ce (YAG) and $Lu_3Al_5O_{12}$ (LuAG) garnets since their invention as phosphors in 60th [6] and cathodoluminescent screens in 70th until recently were overshadowed by more dense and fast Ce or Pr-doped $YAlO_3$ (YAP) [7] and $LuAlO_3$ (LuAP) perovskites [8], as well as more bright Ce-doped orthosilicates

M. Korzhik and A. Gektin (eds.), *Engineering of Scintillation Materials and Radiation Technologies*, Springer Proceedings in Physics 200,
https://doi.org/10.1007/978-3-319-68465-9_7

Lu_2SiO_5 (LSO) [9] and $Lu_{2-x}Y_xSiO_5$ (LYSO) [10]. Luminescence in green spectral range was another drawback of Ce-doped garnets, as it poorly matched the spectral sensitivity range of blue PMTs. The renaissance of Ce-doped garnet scintillators has begun since early 2010th with the progress in crystal production technology of YAG:Ce and LuAG:Ce, as well as the introduction of Gd–Lu-Y/Al-Ga substituted Ce-doped garnets with surprisingly high light output and energy resolution—$Lu_3Al_{5-x}Ga_xO_{12}$ (LuAGG), $Gd_3Al_{5-x}Ga_xO_{12}$, $Gd_{3-x}Y_xAl_{5-x}Ga_xO_{12}$ (GYAGG) L[11–14], etc. In its turn, $Y_3Al_{5-x}Ga_xO_{12}$:Ce (YAGG:Ce) scintillator can be an alternative to the Lu- and Gd-based counterparts. As YAG:Ce, LuAG:Ce, and YAGG:Ce contain light and medium-heavy ions, their radiation hardness to high energy hadrons should be better compared to PWO and other heavy scintillators [15, 16].

Ce^{3+}-doped rare-earth garnets possess relatively long scintillation decay due to a high concentration of defects comprising, first of all, antisite defects and oxygen vacancies, and their aggregates [17, 18], which acting as the luminescent and trapping centers [19, 20] and significantly delay the charge carrier transport to Ce^{3+} luminescence centers [21]. In addition, Al-based garnets possess a very long-wavelengths Ce^{3+} luminescence due to very strong crystal field and large splitting of Ce^{3+} energy levels. It results in relatively slower luminescence decay owing to the fundamental limitation $\tau \sim \lambda^3$ [22] (τ—emission decay time, λ—emission wavelength) in comparison with Ce^{3+} doped orthosilicate and perovskite hosts. These two factors contribute the 60–120 ns decay times of the fast scintillation component in Ce-doped garnets related to the radiative transition within Ce^{3+} ions, and the presence of slower scintillation components with decay times of hundreds of nanoseconds caused by participation of the defects in the excitation of Ce^{3+} luminescence. The slow luminescence decay is a serious drawback, for instance, in HEP application where bunch spacing at colliders could be of 25 ns [1–3].

Introducing of divalent cationic co-dopants became an efficient method to suppress slow decay components in different Ce-doped scintillators, including garnets (see for ex. [23–25]). It is assumed that charge compensation in crystal at substitution of trivalent host rare earth cation (Lu^{3+}, Gd^{3+}, Y^{3+}) with divalent cation (Ca^{2+}, Mg^{2+}) promotes the partial Ce^{3+} transfer into the Ce^{4+} state. It was suggested that tetravalent Ce, previously considered to be a negative factor, competes with other traps for electron capture thus increasing the contribution of fast luminescence [21]. However, decay time shortening in most cases is achieved simultaneously with decreasing of light yield, which falls probably due to ionization of electrons to the conduction band from the excited levels of cerium ion. In this connection the composition-property correlations in YAGG:Ce and issues of its codoping with Ca^{2+} were explored recently [26]. Namely, the light yield around 10,000 phot/MeV and the decay time of 21 ns were achieved in YAGG:Ce,Ca with 75% substitution of Al with Ga in the host. Meanwhile, despite a large number of papers on divalent codoping (see, for ex. [23–26] and references therein) just few of them discuss the issues of the codoping in the μ-PD grown fibers. Unlike bulk crystals, the strong radial segregation of dopants observed in the fibers makes it hard to predict the influence of the codoping on fiber properties and process of their preparation.

Therefore, YAG:Ce—based scintillators possess an attractive combination of high light yield, reasonable density, and fast luminescence decay. Codoping with divalent

cations and bandgap engineering by Al^{3+}/Ga^{3+} substitution provide a possibility of the fine tuning of its scintillation properties according to the practical application requirements. Other serious advantages of garnets comprise a good mechanical robustness, chemical stability, and relatively easy process of their growth in the form of fibers with various shapes. This chapter deals with growth by the μ-PD method and characterization of long YAG:Ce,Mg scintillation fibers. The progress in growth of YAGG:Ce fibers is discussed as well.

2 Experimental

YAG, YAG:Ce, YAG:Ce, Mg, and YAGG:Ce fibers of 2 mm dia. or 2×2 mm^2 cross-section were produced by the μ-PD method at ILM (Lyon, France) by the procedure described elsewhere [5]. Ir crucibles with round (2 mm dia.) and square (2×2 mm^2) capillary dyes, correspondingly, were used for fiber pulling.

After the growth the fibers were cut into the main part with length of 22 cm for attenuation length tests and small (1 cm) parts from the heads and tails of the fibers for measurements of light output and decay time. Meanwhile, some fibers were grown with stepwise change of pulling rate, enabling to cut them into shorter (5–7 cm) fragments, each grown with a certain growth rate.

The light output was measured using samples of 10 mm length by the ^{137}Cs 662 keV source. Integration gate was 1000 ns. Samples were wrapped with Teflon. Optical grease $n \sim 1.5$ was used to couple one end of samples to PMT R2059. Quantum efficiency of PMT was about QE = 9.5% for LuAG:Ce and QE = 7.0% for YAG:Ce. Decay times of scintillation were measured under same excitation using an oscilloscope. Output of the PMT was read-out with a DRS4 unit running at 2 GHz sampling rate and connected to a PC. Since a very low trigger threshold was used to record the pulse shapes, a small percentage of the pulses was originating from single photoelectron noise of the PMT. Such events have been discarded and only the pulses from scintillation were used to calculate the average scintillation waveform. An average of about 1000 pulses is used to obtain the scintillation kinetic of the sample.

Attenuation length L_{att} (i.e., the fiber length where the intensity of LED-excited light falls by e times) was taken as the indicator of fiber optical quality. The attenuation length measurements were carried out using the custom made setup in CERN EP-CMX under excitation with blue light (475 nm) for undoped and Ce-doped fibers. A fast LED driver (SP5601 from CAEN) was used; the light was transported with a clear fiber to the sample. Both extremities of the LuAG and YAG fibers were coupled to SiPms (Model S10931-050P from Hamamatsu). The output of these SiPms were amplified with a dedicated instrumental amplifier (gain of 180) operated in a differential mode. Signals (of both left and right photodetectors) were then acquired with a digitizer (Model DT5720 from CAEN). The fibers were moved with a translating stage (Model M-413.32S from PI).

Cathodoluminescence spectra were measured using transverse polished cuts of the grown fibers. The CL spectra were measured at the room temperature (RT) using an electron microscope SEM JEOL JSM-820 as e-beam source, additionally equipped

with a Ocean Electronics spectrometer and TE-cooled CCD detector working in the 200–925 nm range.

3 Growth and Characterization of YAG:Ce,Mg Fibers

3.1 Growth of YAG:Ce and YAG:Ce,Mg Fibers

YAG:Ce fibers with different dopants concentrations were grown by the μ-PD method. Also we varied the Mg concentration to find the optimal combination of optical and scintillation parameters in YAG:Ce,Mg fibers (Fig. 1). The following growth parameters were varied (Table 1):

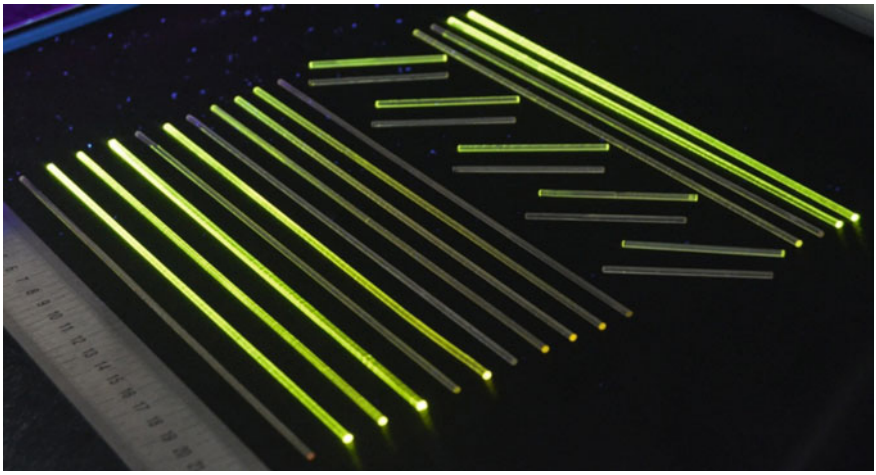

Fig. 1 As-grown fibers of YAG:Ce and YAG:Ce,Mg fibers grown by the μ-PD method under UV-light

- **Concentration of dopants**. YAG and YAG:Ce crystalline chunks were taken as raw materials for fiber growth. Ce concentration in the raw materials was controlled by mixing YAG:Ce with 1000–1200 ppm Ce concentration with undoped YAG. Mg was added to the composition as $MgCO_3$ or MgO powders ("pure for analysis"). The concentrations of Ce and Mg codopants were varied within 100–1000 ppm and 25–120 ppm, correspondingly.
- **Growth atmospheres**. All growth procedures were provided in the Ar-based atmosphere. Apart of "conventional" high purity argon, two types of the custom Ar gas compositions were employed to define possible impact of the gas composition to the process of YAG:Ce,Mg fibers growth. According to manufacturer certificates, these were: (i) Alphagas Ar of 99.999% purity with admixtures of: $H_2O < 3$ ppm, $O_2 < 2$ ppm, organics CnHm < 0.5 ppm; (ii) Arcal Ar of 99.99% purity with admixtures of: $H_2O \leq 5$, $O_2 < 5$, $N_2 < 10$ ppm.

Table 1 Some results on the YAG-based fibers characterization

Sample	Shape	Orientation	Growth rate, mm/min	Ce conc, ppm	Mg conc, ppm	L_{att}, cm,	Light output, photon/MeV (tail/head)	Decay time, ns fast/slow/average,	Gas
YAGC1S	□	111	0.3	1000	–	1.7	20,900/14,900	81/151/132 tail	Ar
YCV1	○	111	0.3	150	–	18	19,900/19,900	72/224/160 tail 58/178/142 head	Ar
YCV2	○	100	0.3	150	–	18	18,900/18,500	89/245/191 tail 93/244/185 head	Ar
YCV3	□	100	0.3	150	–	16.5	20,900/19,900	70/197/143 tail 66/205/157 head	Ar
YCV4	○	111	0.3	150	100	4.5	11,900/11,900	50/126/96 tail 41/120/97 head	Ar
YCV5	○	111	0.3	150	50	12	21,600/21,600	55/190/133 tail 56/198/137 head	Ar
YCV6	○	111	0.3	100	100	2.3	16,200/16,200	46/145/112 tail 44/173/132 head	Ar
YCV7	○	111	0.3	100	50	4.4	18,300/18,300	42/139/111 tail 45/159/117 head	Ar
YCV8	○	111	0.3	100	25	6.5	20,500/20,500	49/156/114 tail 47/165/120 head	Ar
YCV9	○	111	0.3	180	50	5.02	–/–	85/233/180 tail 84/259/196 head	Ar
YCV12	○	111	0.15	150	25	6.58	–/–	96/286/210 head	ALPHAGAS
YCV13	○	111	0.2	180	25	7.59	–/–	118/280/201 tail 119/294/226 head	ARCAL
YCV14	○	111	0.2	200	120	2.63	–/–	110/275/206 tail 113/310/221 head	ALPHAGAS
YCV15	○	111	0.2	150	–	10.07	–/–	120/325/271 head	ALPHAGAS
YCV16	○	111	0.2	150	–	17.96	–/–	–/–/–	ARCAL

- **Growth orientation and shape**. The fibers were grown following [111] and [100] crystallographic orientations of YAG seeds. Fibers with square (2 × 2 mm) and round (2 mm diameter) cross-sections were grown to estimate the influence of the fibers shape on their properties.
- **Pulling rates**. Different fiber pulling rates within the 0.15–0.7 mm/min range were chosen basing on our experience in growth of YAG:Ce and LuAG:Ce fibers [27, 28]. In most cases, each long (>20 cm) fiber was grown with a constant growth rate.

Some of the characterization results are accumulated in Table 1. Light output and luminescence decay times in some fibers were measured in samples cut from different parts of the fiber (tail/head) to check their homogeneity. The presented results show no evidence of fiber growth orientation and shape effect on any measured optical and scintillation parameters. The characteristics were also not sensitive to the origin of raw material and form of co-dopant introduction ($MgCO_3$ or MgO powders). No substantial difference between the properties of samples cut from tails and heads of fibers was noticed. The influence of other growth parameters on fiber properties is discussed hereafter.

3.2 Light Output

The light output in YAG:Ce fibers was around 20,000 photon/MeV independently on Ce concentration in the 100–1000 ppm range (Table 1, Fig. 2). At low Ce-doping the light output in tails/heads is the same within ~5%, while at heavy Ce-doping it is smaller in heads by 30–50%. At Ce, Mg codoping the light output of YAG:Ce falls by up to 40% with increasing Mg concentration (Fig. 2). Therefore, maximal light output in Mg-codoped fibers was achieved at light Ce doping (100–150 ppm) and low Mg concentration.

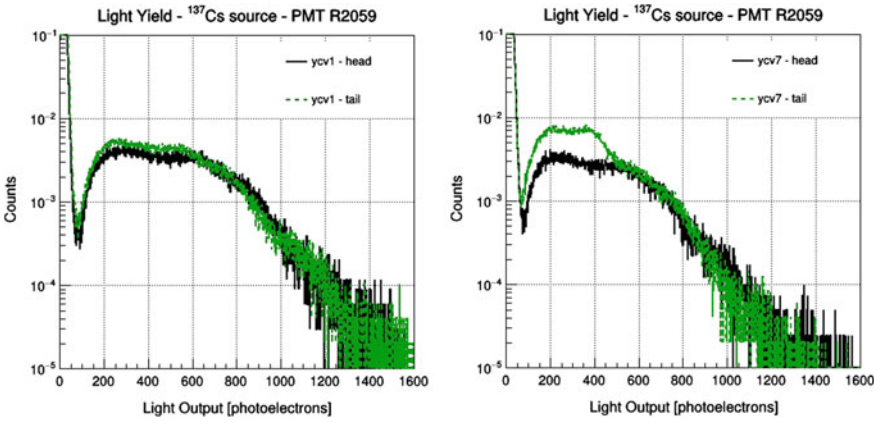

Fig. 2 Amplitude spectra of samples in log scale under excitation with ^{137}Cs 662 keV γ-rays: YAG:Ce (YCV1) and YAG:Ce,Mg (YCV7)

3.3 Decay Time

YAG:Ce fibers with the Ce concentrations of 100–1000 ppm showed similar decay time values. The decay times of fast and slow components at the double-exponential fitting, and the "average" decay times at single-component fitting are 70–120 ns, 180–325 ns, 140–270 ns, correspondingly (Fig. 3). Therefore, the decay times not change despite the 10 times variation of luminescence centers quantity. This is, probably, because the cerium concentration at the fiber periphery where LED light is mainly absorbed is sufficiently high even at light Ce-doping. The decay constants of the samples taken from the heads and tails of the same fibers were similar, which is typical for fibers grown by the μ-PD due to the stable activator distribution along the fiber growth axis. Mg-codoping with the concentrations of 25–120 ppm contributed to the reduction of the scintillation decay times (Fig. 3). The shortest decay time of the fast component was 42 ns in YCV7 fiber containing 100 ppm Ce and 50 ppm of Mg (Mg/Ce ratio = 0.5) (Fig. 3, right). No further decrease of decay times was noticed at the higher Mg/Ce ratios certifying that the ratio Mg/Ce around 0.5 is the optimal from the point of decay time shortening.

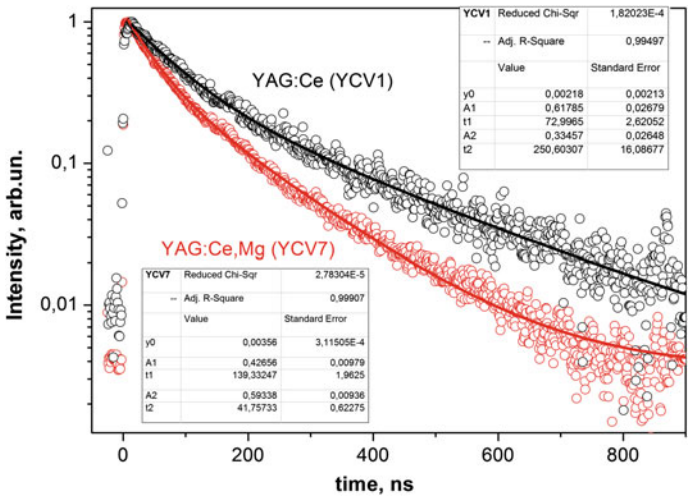

Fig. 3 Luminescence decay of YAG:Ce (YCV1) and YAG:Ce,Mg (YCV7) samples irradiated with ^{137}Cs 662 keV γ-rays. The solid curves are double exponential fits of the experimental points by the function $y = yo + A1\exp(-x/t_1) + A2\exp(-x/t_2)$

3.4 Attenuation Length

Following our experience in growth of YAG:Ce and LuAG:Ce fibers, at heavy Ce doping the fiber periphery is oversaturated with activator and causes the formation of visible macro-defects and cracks, while in the core part of the fibers Ce concentration increase is not significant. This may cause the low attenuation length and claimed the necessity to grow fibers with lower Ce concentrations. The decrease of Ce

concentration in YAG:Ce from 1000 to 100–150 ppm improves the attenuation length from 0.7–0.9 to 16–18 cm. As Mg-codoping reduces the attenuation length, we found that Mg concentration should be within 25–50 ppm, i.e. at the Ce concentration of 100–150 ppm the Ce/Mg ratio should be 0.2–0.3 to minimize the attenuation length deterioration.

As the required length of scintillation fibers for new HEP experiments at colliders should be >40 cm, the obtained attenuation lengths in YAG:Ce,Mg are not enough to provide a good collection of scintillation light. Aiming to further improve the attenuation length the additional experiments were provided to optimize pulling rates of YAG:Ce,Mg fiber growth. Fibers with the same optimized composition were grown with step-by-step variation of pulling rates within 0.15–0.7 mm/min, in order to obtain short samples (L = 5–7 cm) for the characterization.

The diagram of correlation between growth rate and attenuation length in fibers (Fig. 4) shows no obvious tendency. Within the set of samples of this study the best attenuation length of 45 cm was registered in sample grown at 0.3 mm/min. However, this result has not been confirmed with long fibers grown under the same conditions. A tendency to improve the attenuation length in fibers grown under Arcal gas with the largest oxygen concentration can be noted. This evidently points a possible role of oxygen vacancies in deterioration of the attenuation length. The overall large spread of attenuation length values evidences a contribution from some uncontrollable factor(s) affecting thermal conditions in the crystallizer and leading to the formation of inclusions and fiber transparency deterioration.

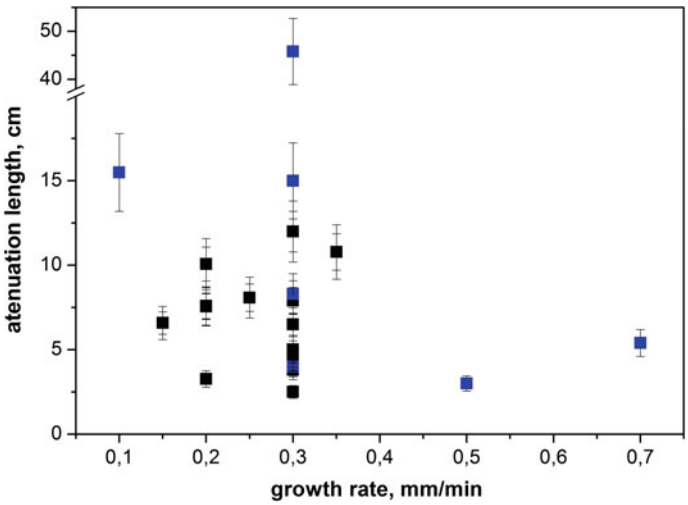

Fig. 4 Correlation between fiber growth rate and measured attenuation lengths in YAG:Ce,Mg fibers. The collected data correspond to the fibers with "optimal" Ce concentration of 100–150 ppm and Mg concentration of 25–50 ppm. Black squares correspond the fibers grown under Ar gas, and blue squares correspond to the fibers grown under Arcal gas

Apart of formation of point lattice defects, such as charged oxygen vacancies and incidental impurities, bad transparency of fibers is attributed to formation of cracks and inclusions due to segregation of Ce^{3+} with large ionic radii to the periphery [27, 29]. The cerium radial distribution can be evaluated by the microscopic image brightness gradient under UV-excitation (Fig. 5). Ce^{3+} luminescence is brighter at the periphery of all the fibers. Meanwhile, the gradient is steeper at 1000 ppm Ce concentration and at Mg-codoping. The homogeneous distribution of activator in YAG:Ce is similar to that observed in prior study of LuAG:Ce with the excellent attenuation length of 104 cm. However, this not contributed to a comparable attenuation length in YAG:Ce. This means that at low Ce-doping the Ce segregation should not be the main cause of bad attenuation lengths in YAG:Ce and YAG:Ce,Mg. As Mg^{2+} was introduced to the melt in the powder form, it may form scattering centers in fibers. Also, in the Mg^{2+}-codoped fibers, Mg^{2+} and Ce^{4+} radial distribution gradient should also affect the optical properties. The presence of cerium mainly in tetravalent state at Mg^{2+}-codoping is certified by visual transparency of Mg^{2+}-containing fiber (Fig. 6), because Ce^{4+} ions, unlike Ce^{3+}, does not possess absorption bands in the visible range [21].

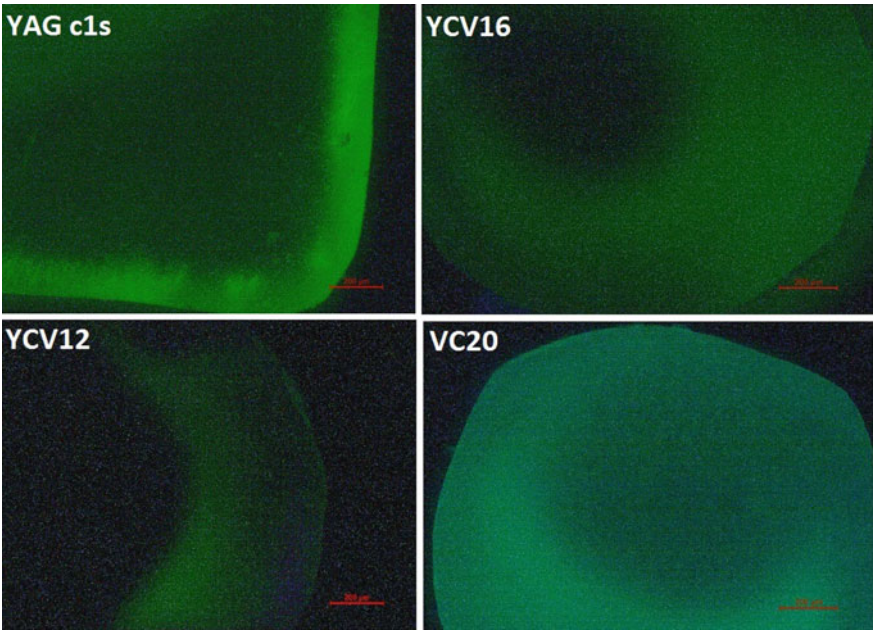

Fig. 5 Photos of transverse sections of YAG:Ce with high (YAGc1s) and low (YCV16) Ce concentration, and YAG:Ce,Mg (YCV12) fibers under LED excitation at 365 nm in comparison with LuAG:Ce fiber with L_{att} = 104 cm obtained in prior study [21] under similar conditions. Concerning the properties of fibers, readers are referred to Table 1

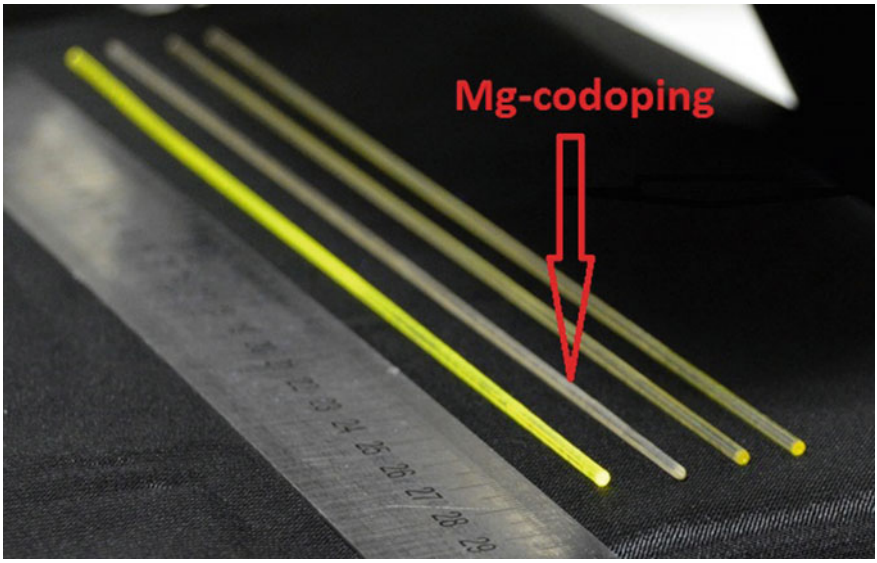

Fig. 6 Photo of as-grown YAG:Ce and YAG:Ce,Mg fibers. While the yellow-green coloration in YAG increases with Ce concentration, the Ce,Mg-codoped fiber (second from the left) is visually transparent likewise undoped YAG due to the $Ce^{3+} \rightarrow Ce^{4+}$ transfer

Cathodoluminescence spectrum of undoped YAG fibers shows the dominant emission band in the UV range related to the Y_{Al} antisite-defect luminescence [30] in the band peaked at 308 nm. In the light and heavy Ce^{3+} doped YAG:Ce fibers the dominant Ce^{3+} emission band peaked at 540 nm are observed (Fig. 7). Cathodoluminescence spectra of the Ce doped fibers at Mg^{2+} codoping demonstrate the strong redistribution of the intensity of Ce^{3+} emission band in the visible range into Y_{Al} antisite defect-related emission band in the UV range. It is worth noting here that Ce^{4+} centers works in parallel with Ce^{3+} emission center and they are not competing in YAG:Ce,Mg [21]. For this reason comparing the intensities of Ce^{3+} luminescence bands of YAG:Ce (YCV1) and YAG:Ce,Mg (YCV4) samples with the same 150 ppm Ce concentration in melt, one can evaluate the fraction of Ce transferred into the tetravalent state. Namely, the mentioned Ce^{3+}/Ce^{4+} ratio in YAG:Ce,Mg (YCV4) garnet is very low and equals approximately to 0.15–0.2. Taking into account also the visual transparency of this sample, we can conclude that the Ce^{4+} is the main valence state of cerium ions in this fiber.

Summarizing, at variation of co-dopants concentrations in YAG:Ce,Mg, the positive effects of decay time decrease at Mg codoping is accompanied by the negative factor of attenuation length decrease. Thus, the reasonable combination of light output and attenuation length in YAG:Ce,Mg was achieved at Ce concentration of 100–150 ppm and Mg/Ce atomic ratio within 0.2–0.5. However, the shortest achieved decay time of 42 ns still not meets the requirements of new HEP experiments at colliders. In this connection the next section describes our efforts to grow YAGG:Ce fibers, because

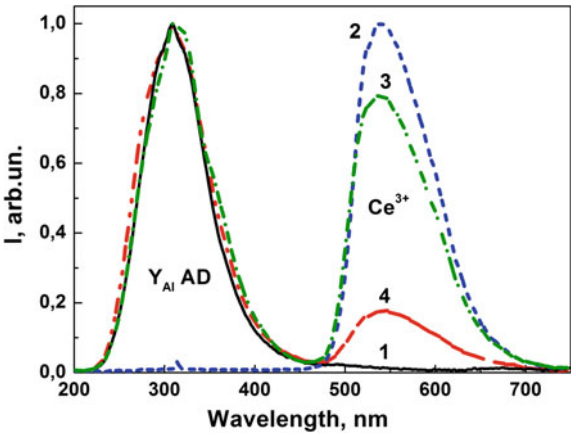

Fig. 7 Normalized CL spectra of fibers: **1** undoped YAG, **2** heavy-doped YAG:Ce (YAGc1 s), **3** low-doped YAG:Ce (YCV1), **4** YAG:Ce,Mg (YCV4)

much shorter decay times of 21–30 ns were demonstrated previously with this material in the form of bulk crystals [26].

4 Growth of YAGG:Ce Fibers

YAGG:Ce fibers with the optimal Ga content of 75 at.% determined in the prior study [26] were grown by the same experimental procedure. The main difference between the YAG and YAGG growth process comprises the non-stoichiometry of melt appearing due to evaporation of volatile Ga oxide. It is a well-known complication at growth of GGG crystals by the Czochralski method [31]. In the micro-PD method the factor of melt evaporation was expected to be more serious, because the melt free surface inside the crucible is open during all the growth process, while in the Czochralski method a part of melt surface is covered with the growing crystal.

A mix of crystalline chunks of YAGG:Ce and YGG crystals grown by the Czochralski method at ISMA [19] was used as raw materials for YAGG fiber growth. In consistency with expectations, the fiber grown from the stoichiometric melt was completely opaque and polycrystalline (Fig. 8). A deficiency of Ga in the melt can be compensated by adding an excess of Ga_2O_3 into the raw material. Following the 1 mol % [31] and 2–4 mol% of Ga_2O_3 [32] excess added to the melt at Czochralski growth of YAGG:Ce and GGG, correspondingly, in the next growth run we added the 3 at.% Ga excess. Despite the shape of new fiber was not perfect, it was transparent and crack-free, except $\sim$1 cm part in the tail. This proved that adding of Ga excess is a proper way to optimize the fiber quality. Choosing further the amount of Ga excess we weighed the amount of gallium oxide deposited on certain parts of the heat insulation (Fig. 9) after growth runs. As no deposit was observed on other parts of the crystallizer, the weight of collected deposit should be close to the amount of evaporated melt. It was determined, that at growth of 4–5 cm long fiber the Ga loss by evaporation is about 10

at.%. Following these data, next fibers were grown from melts with Ga excess 10, 15, 18 at.%—see Fig. 8. Quantity of inclusions decreased with Ga addition. These periodical inclusions, also named as striations, are thickened towards the end of the fibers. Their formation, evidently, is the sequence of melt concentration overcooling due to the large difference of 140 °C between melting temperatures of crystal components [33] –YAG and YGG. Adding of Ga excess over 18 at.% negatively influenced the YAGG:Ce fiber quality.

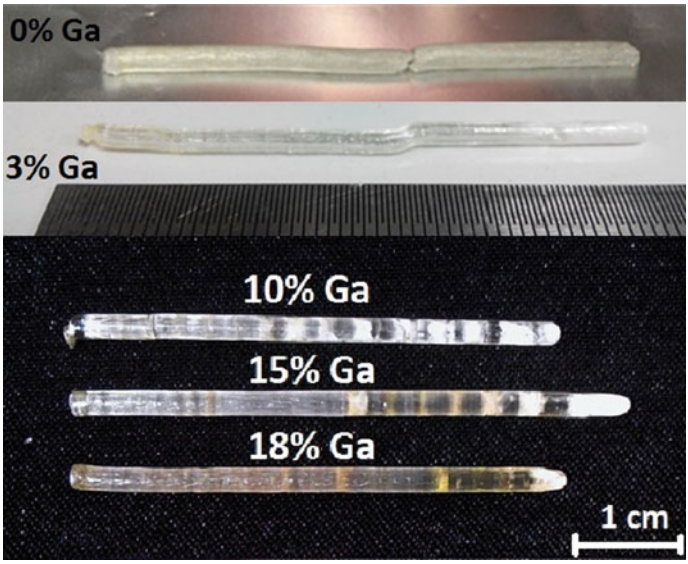

Fig. 8 Photos of as-grown YAGG:Ce fibers with the different Ga excess in the melt. The heads (beginnings) of fibers are on the left

Thus, the YAGG:Ce fiber growth process by the μ-PD method is severely complicated by the uncontrollable Ga_2O_3 evaporation, and periodical striations called by constitutional supercooling in the mixed YAG:Ce – YGG:Ce system. As gallium oxide losses by evaporation are nearly proportional to the growth process duration, they will be much larger at growth of long fibers with the required length of >20 cm. These losses can be minimized by adding larger amount of oxygen into growth atmosphere, or insulating the melt from the environment. The striations should be avoided by the decrease of fiber growth rate, which, in turn, questions a possibility of YAGG:Ce mass production in reasonable terms.

Fig. 9 Ga oxide deposited at the heat insulation after YAGG fiber growth by the micro-PD method. The lower photo represents the deposit collected into a test-tube

5 Conclusions

Long (>20 cm) YAG:Ce,Mg scintillation fibers were grown by the μ-PD method. At the optimal Ce concentration 100–150 ppm and Mg concentration 25–50 ppm the light output of around 15,000–20,000 phot/MeV, decay time of 42 ns, and attenuation length up to 16 cm were achieved. The attenuation length of 45 cm was determined with shorter (5 cm long) fiber, but has not been confirmed with long fibers. Accounting for the optical and scintillation properties and the need to reduce the time needed for fiber production, the 0.3 mm/min pulling rate looks as a reasonable compromise for YAG:Ce,Mg—fibers.

The achieved scintillation decay times are still too long to match the requirements (τ = 25–40 ns) of new HEP experiments at colliders, and there is no reproducible procedure to obtain the long fibers with the required attenuation length >40 cm. The further optimization of codopants concentrations and growth conditions is under way.

A feasibility to grow straight and transparent YAGG:Ce fibers by the micro-PD method is shown. However, huge Ga_2O_3 losses and striations formed in these fibers make it hardly possible to develop a method to fabricate the long fibers with a reasonable and reproducible quality.

Acknowledgements. This work was performed in the framework of the Crystal Clear Collaboration and received funding from the European Union's Horizon 2020 research and innovation program under the Marie Skodowska-Curie grant agreement no. 644,260 (Intelum) and Polish NCBR NANOLUX#286 project. The Ukrainian and French teams also acknowledge the support from Ukrainian-French PICS project between CNRS (Project no.6598) and National Academy of Sciences of Ukraine (Project F1-2017). Authors are grateful to Dr. Martin Nikl (Institute of Physics AS CR, Prague, Czech Republic) and Dr. Ashot Petrosyan (Institute for

Physical Research, National Academy of Sciences, Ashtarak, Armenia) for providing the raw materials for this study.

References

1. G. Mavromanolakis, E. Auffray, P. Lecoq, Studies on sampling and homogeneous dual readout calorimetry with meta-crystals. J. Instrum. **6**, P10012 (2011)
2. M. Lucchini, T. Medvedeva, K. Pauwels et al., Test beam results with LuAG fibers for next-generation calorimeters. J. Instrum. **8**, P10017 (2013)
3. A. Benaglia, M. Lucchini, K. Pauwels et al., Test beam results of a high granularity LuAG fibre calorimeter prototype. J. Instrum. **11**, P05004 (2016)
4. M. Vasilyev, Neutron and gamma sensitive fiber scintillators. US Patent 9,482,763, 1 Nov 2016
5. K. Lebbou, Single crystals fiber technology design. Where we are today? Opt. Mater. **63**, 13–18 (2017)
6. G. Blasse, A. Bril, A new phosphor for flying-spot cathode-ray tubes for color television: yellow-emitting Y3al5o12–Ce3. Appl. Phys. Lett. **11**, 53–55 (1967)
7. V.G. Baryshevsky, M.V. Korzhik, V.I. Moroz et al., YAlO3: Ce-fast-acting scintillators for detection of ionizing radiation. Nucl. Instrum. Methods Phys. Res. Sect. B **58**, 291–293 (1991)
8. B.I. Minkov, Promising new lutetium based single crystals for fast scintillators. Funct. Mater. **1**, 103–105 (1994)
9. C.L. Melcher, J.S. Schweitzer, A promising new scintillator: cerium-doped lutetium oxyorthosilicate. Nucl. Instrum. Methods Phys. Res. Sect. A **314**, 212–214 (1992)
10. D.W. Cooke, K.J. McClellan, B.L. Bennett et al., Crystal growth and optical characterization of cerium-doped Lu 1.8 Y 0.2 SiO 5. J. Appl. Phys. **88**, 7360–7362 (2000)
11. T. Kamada, K. Endo, T. Tsutumi et al., Composition engineering in cerium-doped (Lu, Gd) 3 (Ga, Al) 5O12 single-crystal scintillators. Cryst. Growth Des. **11**, 4484–4490 (2011)
12. K. Kamada, S. Kurosawa, P. Prusa et al., Cz grown 2-in. size Ce: Gd 3 (Al, Ga) 5 O 12 single crystal; relationship between Al, Ga site occupancy and scintillation properties. Opt. Mater. **36**, 1942–1945 (2014)
13. C. Wang, Y. Wu, D. Ding, Optical and scintillation properties of Ce-doped (Gd2Y1) Ga2.7Al2.3O12 single crystal grown by Czochralski method. Nucl. Instrum. Methods Phys. Res. Sect. A **820**, 8–12 (2016)
14. A. Giaz, G. Hull, V. Fossati et al., Preliminary investigation of scintillator materials properties: SrI2:Eu, CeBr 3 and GYGAG: Ce for gamma rays up to 9 MeV. Nucl. Instrum. Methods Phys. Res. Sect. A **804**, 212–220 (2015)
15. E. Auffray, A. Barysevich, A. Fedorov et al., Radiation damage of LSO crystals under γ-and 24 GeV protons irradiation. Nucl. Instrum. Methods Phys. Res. Sect. A **721**, 76–82 (2013)
16. E. Auffray, A. Barysevich, A. Gektin et al., Radiation damage effects in Y2SiO5: Ce scintillation crystals under γ-quanta and 24 GeV protons. Nucl. Instrum. Methods Phys. Res. Sect. A **783**, 117–120 (2015)
17. Y. Zorenko, Luminescence of isoelectronic impurities and antisite defects in garnets. Phys Stat Sol C **2**, 375–379 (2005)
18. C. Stanek, K. McClellan, M. Levy et al., The effect of intrinsic defects on RE3Al5O12 garnet scintillator performance. Nucl. Instrum. Methods Phys. Res. Sect. A **579**, 27–30 (2007)

19. M. Nikl, E. Mihokova, J. Pejchal et al., The antisite LuAl defect-related trap in Lu3Al5O12: Ce single crystal. Phys. Stat. Sol. B **242**, R119–R121 (2005)
20. Y. Zorenko, V. Gorbenko, I. Konstankevych et al., Single-crystalline films of Ce-doped YAG and LuAG phosphors: advantages over bulk crystals analogues. J. Lumin. **114**, 85–94 (2005)
21. P. Dorenbos, Light output and energy resolution of Ce 3 + -doped scintillators. Nucl. Instrum. Methods Phys. Res. Sect. A **486**, 208–213 (2002)
22. K. Kamada, M. Nikl, S. Kurosawa et al., Alkali earth co-doping effects on luminescence and scintillation properties of Ce doped $Gd_3Al_2Ga_3O_{12}$ scintillator. Opt. Mater. **41**, 63–66 (2015)
23. Y. Wu, F. Meng, Q. Li et al., Role of Ce^{4+} in the scintillation mechanism of codoped $Gd_3Ga_3Al_2$ O_{12} Ce. Phys. Rev. Appl. **2**, 044009 (2014)
24. A. Nagura, K. Kamada, M. Nikl et al., Improvement of scintillation properties on Ce doped Y3Al5O12 scintillator by divalent cations co-doping. Jpn. J. Appl. Phys. **54**, 04DH17 (2015)
25. M. Nikl, K. Kamada, V. Babin et al., Defect engineering in Ce-doped aluminum garnet single crystal scintillators. Cryst. Growth Des. **14**, 4827–4833 (2014)
26. O. Sidletskiy, I. Gerasymov, D. Kurtsev, Engineering of bulk and fiber-shaped YAGG: Ce scintillator crystals. Cryst. Eng. Comm. **19**, 1001 (2017)
27. V. Kononets, E. Auffray, C. Dujardin et al., Growth of long undoped and Ce-doped LuAG single crystal fibers for dual readout calorimetry. J. Cryst. Growth **435**, 31–36 (2016)
28. A. Djebli, F. Boudjada, K. Pauwels, Growth and characterization of Ce-doped YAG and LuAG fibers. Opt. Mater. **65**, 66–68 (2016)
29. V. Kononets, O. Benamara, G. Patton, Growth of Ce-doped LGSO fiber-shaped crystals by the micro pulling down technique. J. Cryst. Growth **412**, 95–102 (2015)
30. Y. Zorenko, A. Voloshinovskii, V. Savchyn et al., Exciton and antisite defect-related luminescence in $Lu_3Al_5O_{12}$ and $Y_3Al_5O_{12}$ garnets. Phys. Stat. Sol. B **244**, 1289–2180 (2007)
31. J. Carruthers, M. Kokta, R. Barns et al., Nonstoichiometry and crystal growth of gadolinium gallium garnet. J. Cryst. Growth **19**, 204–208 (1973)
32. O. Sidletskiy, V. Kononets, K. Lebbou et al., Structure and scintillation yield of Ce-doped Al–Ga substituted yttrium garnet. Mater. Res. Bull. **47**, 3249–3252 (2012)
33. C. Brandle, A. Valentino, Czochralski growth of rare earth gallium garnets. J. Cryst. Growth **12**, 3–8 (1972)